ACCSCIENCE PUBLISHING

Asian Journal of Water, Environment and Pollution

ORIGINAL RESEARCH ARTICLE

Broadband shear wave velocity profiling to evaluate subsidence vulnerability: A combined multichannel analysis of surface waves approach in Quang Ninh, Vietnam

Nguyen Nhat Kim Ngan[1,2]*, Nguyen Thanh Hai[3,4], and Nguyen Van Thuan[1,2]

[1]Department of Geophysics, Faculty of Physics and Engineering Physics, University of Science, Ho Chi Minh City, Vietnam

[2]Vietnam National University, Ho Chi Minh City, Vietnam

[3]Department of Seismology, Institute of Earth Sciences, Hanoi, Vietnam

[4]Viet Nam Academy of Science and Technology, Hanoi, Vietnam

Abstract

As urban centers expand into geologically complex and hazardous terrains, accurately characterizing deep subsurface stiffness becomes critical for disaster mitigation. Traditional active multichannel analysis of surface waves (MASW) provides excellent near-surface resolution but struggles to penetrate beyond 30 m. Conversely, passive MASW captures deep geological interfaces but lacks high-frequency data for shallow soil profiling. We addressed this limitation by deploying a combined active and passive MASW framework to extract broadband dispersion curves (2–11 Hz) in Quang Hanh, Quang Ninh Province, Vietnam—a region currently facing severe subsidence risks. Seismic data were acquired using a fixed 24-channel array (3 m spacing, 69 m length) utilizing both a sledgehammer source and ambient urban noise. Data processing was conducted using ParkSEIS v2.0, applying a phase-shift algorithm for active data and the extended spatial autocorrelation method for passive data. Through constrained iterative least-squares inversion, we generated one-dimensional shear wave velocity profiles down to a depth of 50 m. The results revealed a highly distinct stratigraphic profile correlating with local borehole data: a semi-stiff clayey topsoil (m/s), a transition zone (m/s), and a basal layer of fractured limestone (m/s). The time-averaged shear wave velocity of 408–517 m/s classifies the area as National Earthquake Hazards Reduction Program site class C. Crucially, the results identified a sharp impedance contrast at the 15 m soil–rock interface. This structural discontinuity indicates a zone of high susceptibility to internal erosion (piping) within the fractured limestone, significantly elevating the risk of karst sinkholes during extreme weather events. This study demonstrates that integrating active and passive MASW provides a robust, non-destructive diagnostic tool for engineers to assess deep geohazards in complex transitional geologies.

Keywords: Geohazards; Karst; Multichannel analysis of surface waves; Shear wave velocity; Subsurface characterization

***Corresponding author:**
Nguyen Nhat Kim Ngan
(nnkngan@hcmus.edu.vn)

Citation: Ngan NNK, Hai NT, Thuan NV. Broadband shear wave velocity profiling to evaluate subsidence vulnerability: A combined multichannel analysis of surface waves approach in Quang Ninh, Vietnam. *Asian J Water Environ Pollut*. 2026;23(4):026170114. doi: 10.36922/AJWEP026170114

Received: March 23, 2026

Accepted: May 18, 2026

Published online: June 10, 2026

1. Introduction

Geotechnical engineers and urban planners continuously face the challenge of securing infrastructure in environments prone to geological hazards. As metropolitan areas expand into geologically complex zones, understanding the dynamic properties of the subsurface becomes paramount. Investigators rely heavily on the shear wave velocity as a fundamental parameter to evaluate soil stiffness, predict seismic site response, and assess foundation bearing capacity. Traditional invasive methods, such as standard penetration tests (SPT) and downhole seismic surveys, yield highly accurate, depth-specific data. However, they remain expensive, time-consuming, and spatially restricted. To overcome these logistical barriers, geophysicists have increasingly turned to non-destructive surface wave methods.

Introduced in the late 1990s, active multichannel analysis of surface waves (MASW) revolutionizes near-surface exploration by analyzing the dispersive properties of Rayleigh waves.[1,2] When a seismic impact is generated on the ground surface, the resulting Rayleigh waves travel at different velocities depending on their wavelengths. By recording these waves with a linear geophone array and transforming the time–space data into the phase velocity–frequency domain, a dispersion image is generated. The fundamental mode of this dispersion curve is then inverted to construct a one-dimensional (1D) profile. Active MASW excels in characterizing the top 15–30 m of the subsurface. However, the energy generated by a standard sledgehammer rapidly attenuates. Consequently, active MASW frequently fails to produce the low-frequency signals (<7 Hz) required to map deeper bedrock interfaces or investigate deep-seated geohazards.[3]

To bridge this depth gap, researchers employ passive MASW. Instead of relying on an artificial impact, the passive approach harnesses ambient microtremors generated by natural phenomena and cultural activities.[4] These ambient vibrations inherently possess low frequencies, allowing them to penetrate depths exceeding 50 m.[5,6] Yet, passive MASW carries its own critical limitation: it often lacks the high-frequency energy necessary to resolve the shallowest soil layers.[7] If engineers rely solely on passive data, they risk overlooking the soft, unconsolidated topsoils that directly interact with shallow foundations.

Recognizing that neither method alone provides a complete picture of a complex subsurface, combining active and passive MASW offers a synergistic solution.[8] By recording active impacts and ambient noise using the same receiver array, geophysicists can merge the high-frequency dispersion data from the active survey with the low-frequency data from the passive survey.[9,10] This integration yields a continuous, broadband dispersion curve. Over the past two decades, researchers worldwide have successfully applied this combined methodology to map deep bedrock topography,[11,12] characterize soft marine clay deposits,[13] investigate fault zones,[14] characterize landfills and embankments,[15,16] evaluate post-earthquake site conditions,[17] conduct seismic microzonation in highly urbanized areas,[18,19] compare local site conditions,[20] map active fault lines,[21,22] characterize embankments and foundation stability,[23,24] and evaluate specific industrial zones.[25] Despite its proven global efficacy, the combined MASW approach remains notably underutilized in Vietnam. Most domestic geophysical investigations still rely exclusively on active MASW or traditional seismic methods, effectively blinding engineers to deeper geological vulnerabilities.[26,27]

This technological gap is particularly alarming in regions like Quang Ninh Province, Vietnam. The specific geological context of our study area, Quang Hanh Ward, features a highly complex transitional topography where coastal plains abruptly meet low mountain ranges. Geologically, the area sits at the boundary of the Hon Gai Formation (sandstone and siltstone) and the Bac Son Formation (massive, yet highly fractured limestone). This karst environment is notorious for internal erosion, subterranean cavities, and sudden sinkhole collapses. Furthermore, climate change continues to intensify the region's vulnerability. Recent extreme weather events, notably Typhoon Yagi, have triggered severe flooding, abruptly altering groundwater levels and initiating landslides.[28] Assessing this specific geohazard susceptibility requires mapping not just the shallow clay, but the deep soil-rock interface accurately.

Therefore, this study aims to validate the efficacy of the combined active and passive MASW method in a challenging, landslide-prone, and high-risk geological setting.[29] Our primary objectives are fourfold: First, to acquire high-quality broadband dispersion data using a linear 24-channel array in an urbanized karst terrain. Second, to invert this data to generate continuous 1D profiles extending to a depth of at least 50 m. Third, to correlate these non-destructive geophysical profiles directly with invasive borehole data to prove the method's accuracy. Finally, to investigate how the derived geotechnical parameters illuminate the underlying mechanics of subsidence susceptibility in Quang Hanh.

2. Materials and methods

2.1. Geological context and site characterization

We conducted this investigation in Group 7, Zone 5, Quang Hanh Ward, Cam Pha City, Quang Ninh Province, Vietnam. Stratigraphically, the survey area lies exactly at the geological boundary between two distinct formations: the upper weathered residual clays of the Hon Gai Formation and the underlying light- to dark-gray limestone of the Bac Son Formation. This limestone is not intact; tectonic activities and chemical weathering have rendered it highly fragmented and karstified.[28] A conceptual illustration of this typical karst topography is presented in Figure 1.

Prior to geophysical data acquisition, we analyzed existing geotechnical borehole logs from the site. The planar distances between the reference boreholes and the two geophysical survey lines range from 25 to 125 m. Given the regional tectonic setting, the stratigraphic layers in this area exhibit strong lateral continuity, making the borehole data a highly reliable reference. As summarized in Table 1, the borehole data reveal a top 9–10 m of semi-stiff to stiff clayey soils with SPT N-values ranging from 4 to 17. Directly beneath this clay layer, the drill bit encountered hard, fragmented limestone.

2.2. Seismic data acquisition strategy

To capture a broadband surface-wave spectrum, we deployed a fixed linear array consisting of 24 vertical-component geophones, each with a natural frequency of 4.5 Hz, connected to a 24-channel GEODE seismograph (UBC Vs30/IBC Vs100, Geometrics Inc., USA). We established two primary survey lines (Site 1 and Site 2) adjacent to the reference borehole (Figure 2).

Array geometry justification: For both sites, we maintained a uniform receiver spacing of 3.0 m, resulting in a total active array length of 69 m. This specific geometry was theoretically designed to achieve the target detection depth of 50 m. According to the empirical relationship in surface wave surveying, the reliable investigation depth is approximately half of the longest reliable wavelength.[3,11]

The maximum wavelength is related to the phase velocity and the minimum frequency dictated by the geophone. Based on the passive dispersion images acquired in this region, phase velocities at low frequencies (approximately 2 Hz) generally exhibit < 500 m/s. Substituting these values into **Equation 1** yields a reliable exploration depth of 55.5 m, which perfectly accommodates our 50-m target depth requirement. Substituting into **Equation 2** yields 111 m. The field setup is depicted in Figure 3.

Active data acquisition: We generated the active seismic source by vertically striking a 10 kg sledgehammer against a metal plate with a 9.0 m source offset. The sampling interval was 0.5 ms with a recording time of 250 ms. We stacked records from five consecutive hammer strikes to enhance the signal-to-noise ratio (SNR).

Passive data acquisition: Immediately following the active shots, we recorded passive microtremors using the exact same fixed linear array. The passive source consisted of ambient vehicular traffic. We recorded continuous blocks of data for 30–60 s at a 2.0 ms sampling interval. Recording durations of 30–60 s are statistically sufficient to capture a stable and representative ambient wavefield in urban environments.[8]

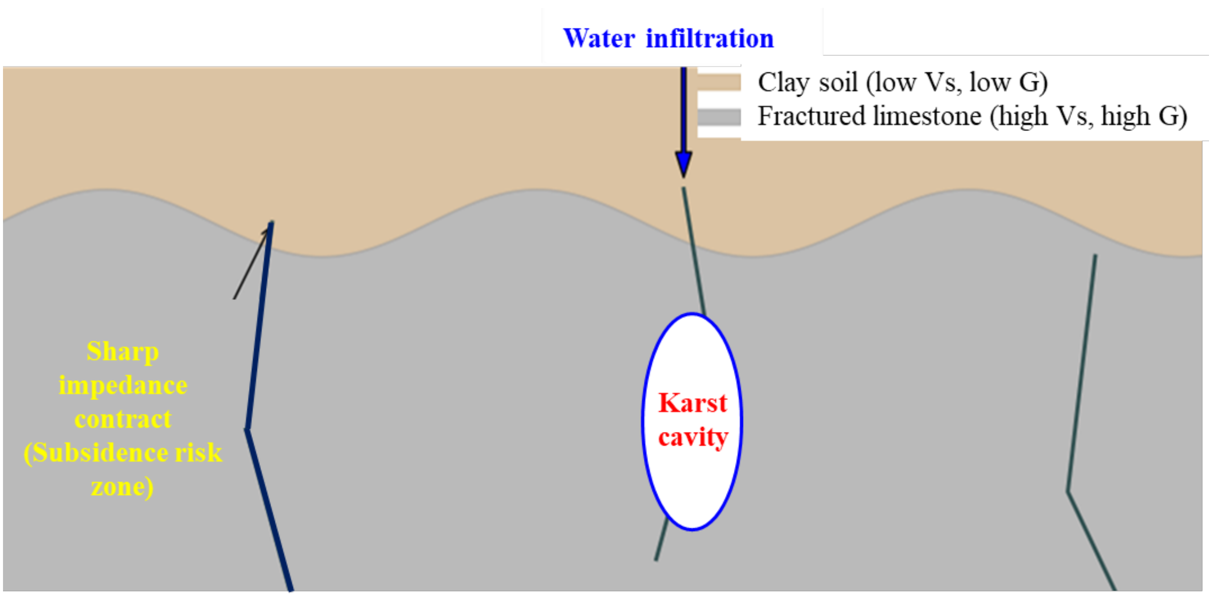

Figure 1. Conceptual geological cross-section illustrating the typical karst topography in the Quang Hanh area, highlighting the interface between the unconsolidated clayey overburden and the fractured limestone bedrock susceptible to piping

Abbreviation: Vs: Velocity.

Table 1. Generalized stratigraphic column of the study area based on reference borehole logging

Layer no.	Approximate depth (m)	Lithological description	Average density (ρ, kg/m³)	SPT N-value range	Inferred geotechnical condition
1	0.0–6.8	Grayish brown, grayish yellow, semi-stiff clayey soil	1.81	4–7	Unconsolidated, soft overburden
2	6.8–9.0	Brownish yellow, grayish yellow, semi-stiff, clayey soil	1.89	~17	Transition zone, increasing stiffness
3	> 9.0 (to 30.0)	Dark gray, fragmented and fractured limestone, hard rock (Bac Son formation)	2.53	N/A (bedrock)	Highly rigid, potential karstification

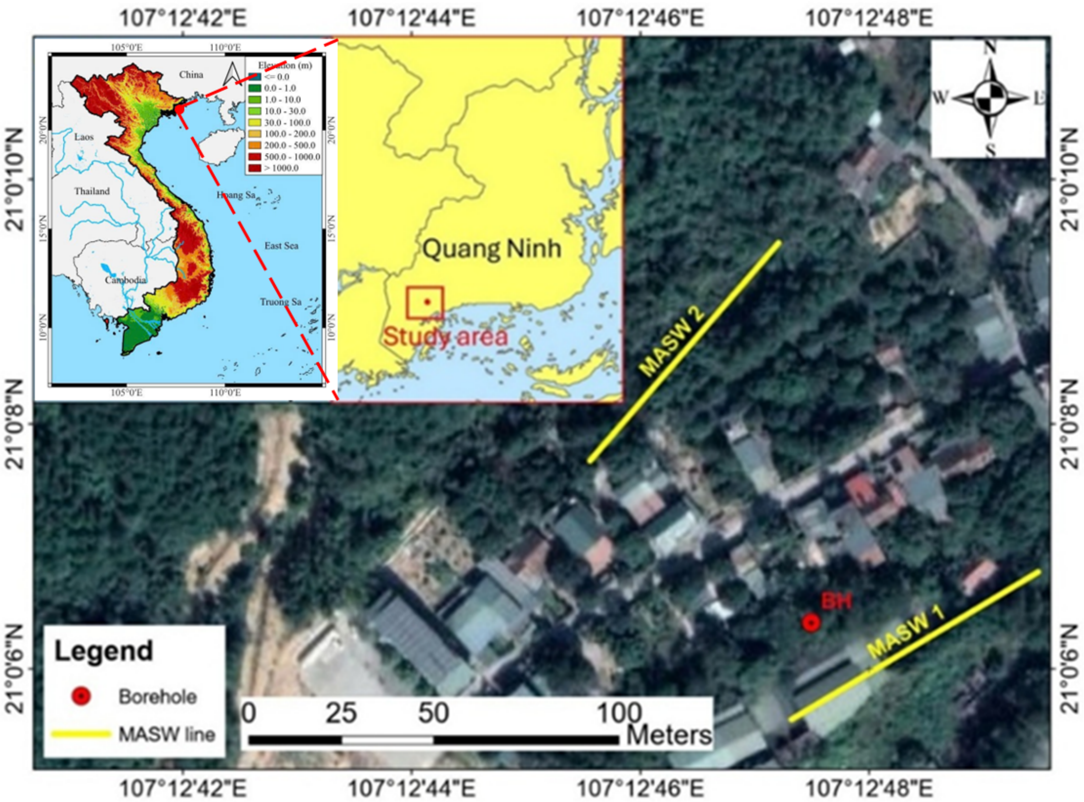

Figure 2. Location of the two multichannel analysis of surface wave (MASW) survey lines (Site 1 and Site 2) and the reference geological borehole within the study area in Quang Hanh, Vietnam

2.3. Data processing and dispersion analysis

We processed the raw seismic data using the ParkSEIS (v2.0, Park Seismic LLC, USA) software suite to transform the records from the time-distance domain into the phase velocity–frequency domain.

Active data processing: A standard phase-shift wavefield transformation technique was applied to decompose the multichannel record into individual frequency components using a fast Fourier transform.

Passive data processing: We employed the extended spatial autocorrelation (ESPAC) method. While traditional spatial autocorrelation relies on circular arrays, ESPAC is a more flexible extension that allows arbitrary receiver geometries, including the linear array used in this study.[4,6] ESPAC effectively handles omnidirectional ambient

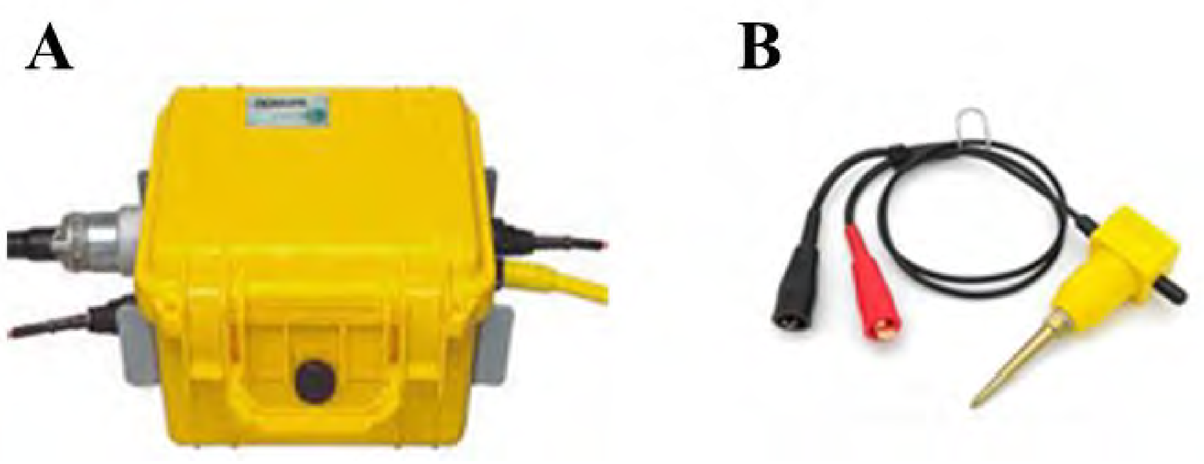

Figure 3. Seismic data acquisition equipment: (A) 24-channel GEODE seismograph and (B) 4.5 Hz vertical geophones utilized in both active and passive multichannel analysis of surface wave surveys

noise and improves the resolution of long wavelengths critical for deep profiling. Furthermore, because passive sources (vehicular traffic) generate off-line and cylindrical wavefronts, the ESPAC method inherently accounts for omnidirectional wave propagation.[4,8] This mathematical framework effectively mitigates the phase velocity overestimation that typically occurs when assuming strictly inline planar waves in standard processing.

Fusion and stacking strategy: The active and passive source data were fused in the frequency–wavenumber domain using a cross-correlation-based stacking method.[30] To avoid dispersion curve shifts caused by massive energy differences between the sledgehammer impact and the ambient noise, a normalization step was performed.[7] The power spectrum of each dataset was normalized by its maximum absolute amplitude at each frequency prior to summation. This statistical stacking significantly increased the SNR, creating a single, continuous broadband dispersion curve (Figure 4).

Dispersion curve picking and uncertainty control: The fundamental mode of the Rayleigh wave was extracted using a semi-automatic picking algorithm in ParkSEIS. To control subjective bias and systematically constrain picking errors, theoretical "bounds" (upper and lower limits of phase velocity at specific frequencies) were predefined within the software. These bounds served as a strict error-range control, preventing the algorithm from tracking false extreme values caused by ambient noise artifacts. To further evaluate uncertainties, a rigorous consistency check was applied: Only data points with excellent signal quality (SNR quality score ≥ 86%) as evaluated by the software during extraction were retained for inversion.

2.4. Inversion algorithm and geotechnical parameterization

An iterative least-squares inversion was used to estimate the 1D shear wave velocity profile. Because surface wave inversion inherently suffers from non-uniqueness, strict parameter constraints were applied based on *a priori* local borehole data.

During the inversion process, the parameters were treated as follows:

(i) Fixed parameters: The number of layers (set to 10 variable depths up to 50 m), layer thicknesses, Poisson's ratio for soils (for bedrock), and mass density. The density was fixed at 1.81–1.89 for the clay layers and 2.53 for the limestone, based directly on the geotechnical logs.
(ii) Inverted parameter: The shear wave velocity was the sole parameter inverted and adjusted iteratively. The inversion process iterated until the root mean square error (RMSE) between the theoretical and measured dispersion curves fell below a 5% convergence threshold. To evaluate the engineering implications, we calculated three critical geotechnical parameters:

- Time-averaged shear wave velocity (**Equation 1**):

$$V_{S30} = \frac{30}{\sum_{i=1}^{n} \frac{h}{V_{Si}}} \quad (1)$$

where h_i is the thickness (in m) and V_{si} is the shear wave velocity (in m/s) of the i-th layer within the top 30 m.[17,21]

- Dynamic shear modulus: Sensitivity analyses

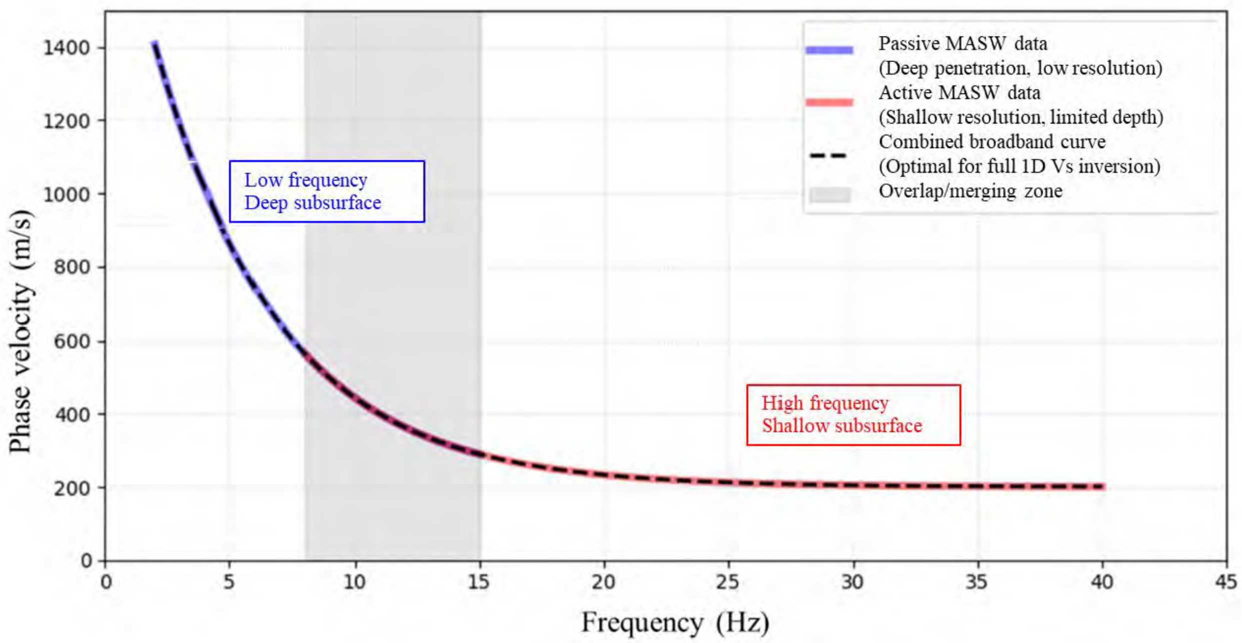

Figure 4. Schematic representation of the combined MASW methodology. The high-frequency active dispersion data (resolving the shallow subsurface) merges with the low-frequency passive dispersion data (penetrating the deep subsurface) to form a comprehensive broadband dispersion curve. Abbreviations: 1D: One-dimensional; MASW: Multichannel analysis of surface wave; Vs: Velocity.

indicate that variations in dominate the value calculation due to the squared relationship, making the fixed borehole density values sufficiently reliable. We calculated the dynamic shear modulus (G), a highly important elastic parameter,[13,29] as in **Equation 2**:

$$G = \rho \cdot V_S^2 \tag{2}$$

where ρ is the bulk density of the soil layer (in kg/m^3).

- Ground predominant period: This parameter is calculated for multi-layered media assuming interface reflections.[29] We estimated the ground predominant period (T_s) using **Equation 3:**[10]

$$T_S = \sum_{i=1}^{n} \frac{4h_i}{V_{Si}} \tag{3}$$

3. Results

3.1. Dispersion image analysis

The raw seismic records and the resulting dispersion transformations clearly demonstrate the necessity of the combined approach. Figure 5 presents the active and passive seismic records for Site 1, while Figure 6 illustrates the sequential generation of dispersion images. Correspondingly, Figures 7 and 8 present the data for Site 2.

When analyzing the active MASW dispersion images (Figures 6A and 8A), high-energy signals dominate the higher-frequency spectrum (above 5–7 Hz), effectively resolving shallow clay layers. However, the fundamental mode is entirely absent below 5 Hz, rendering the active method blind to the deeper bedrock. Conversely, the passive ESPAC dispersion images (Figures 6B and 8B) exhibit massive energy concentrations in the low-frequency domain down to 2 Hz. By stacking the normalized matrices, we produced the combined dispersion images (Figures 6C and 8C). This integration seamlessly bridged the frequency gap. We confidently selected the peak amplitudes along this broadband curve (Figures 6D and 8D) as the input for the inversion process.

3.2. Shear wave velocity profiles and derived parameters

The constrained iterative inversion yielded robust 1D profiles extending to 50 m. Figure 9 displays the inverted structures (blue lines) alongside the theoretical (blue dots) and measured (red dots) dispersion curves, confirming the RMSE < 5% convergence.

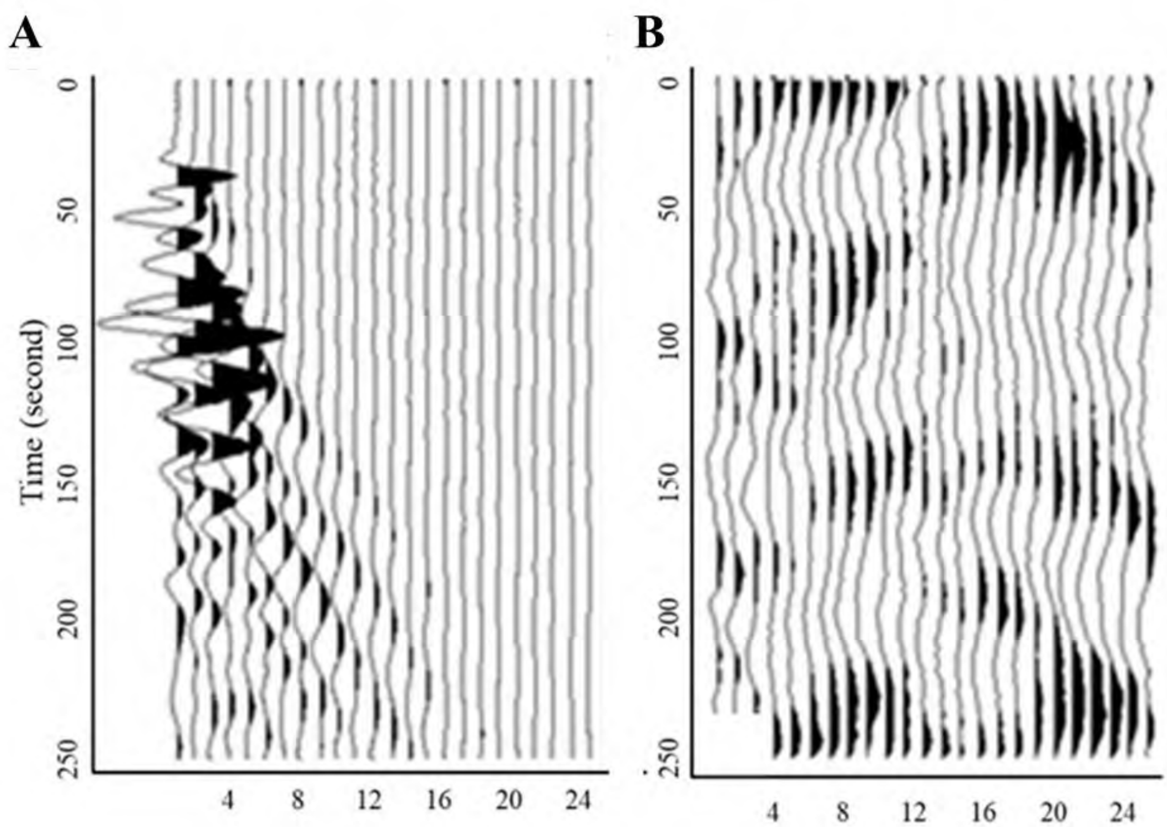

Figure 5. Raw seismic records for (A) the active multichannel analysis of surface wave (MASW) survey (250 ms) and (B) the passive MASW survey (>30 s block) at Site 1

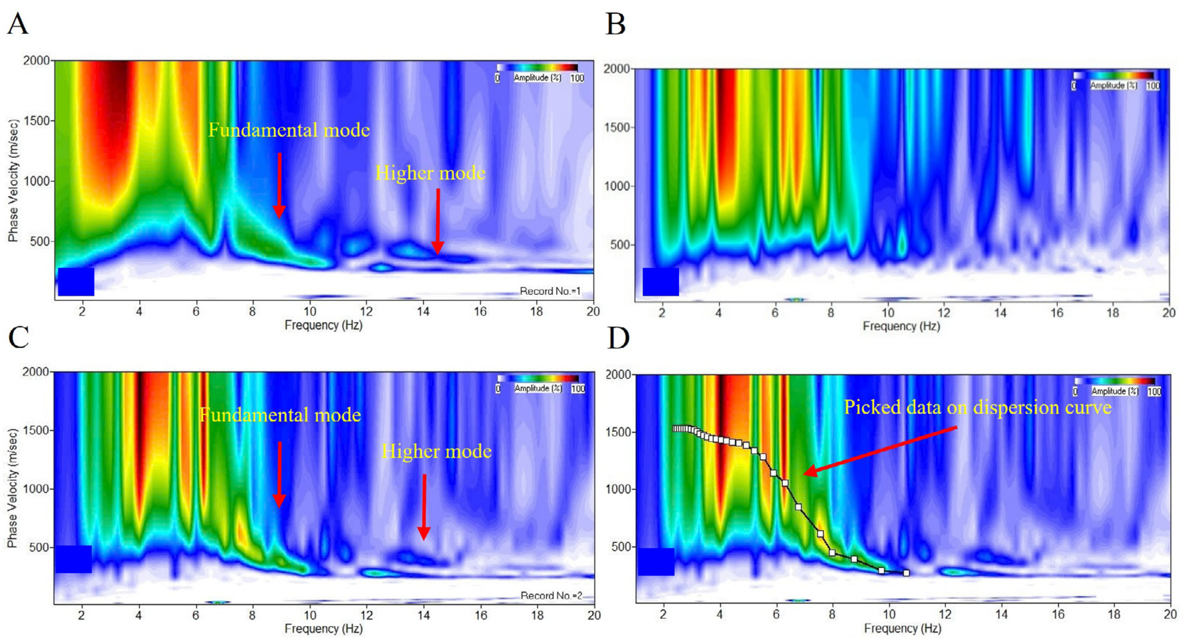

Figure 6. Dispersion images from Site 1. (A) Active multichannel analysis of surface wave data. (B) Passive extended spatial autocorrelation data. (C) The stacked combined data in the domain. (D) The combined data with the picked fundamental mode (white squares) constrained by theoretical upper and lower bounds.

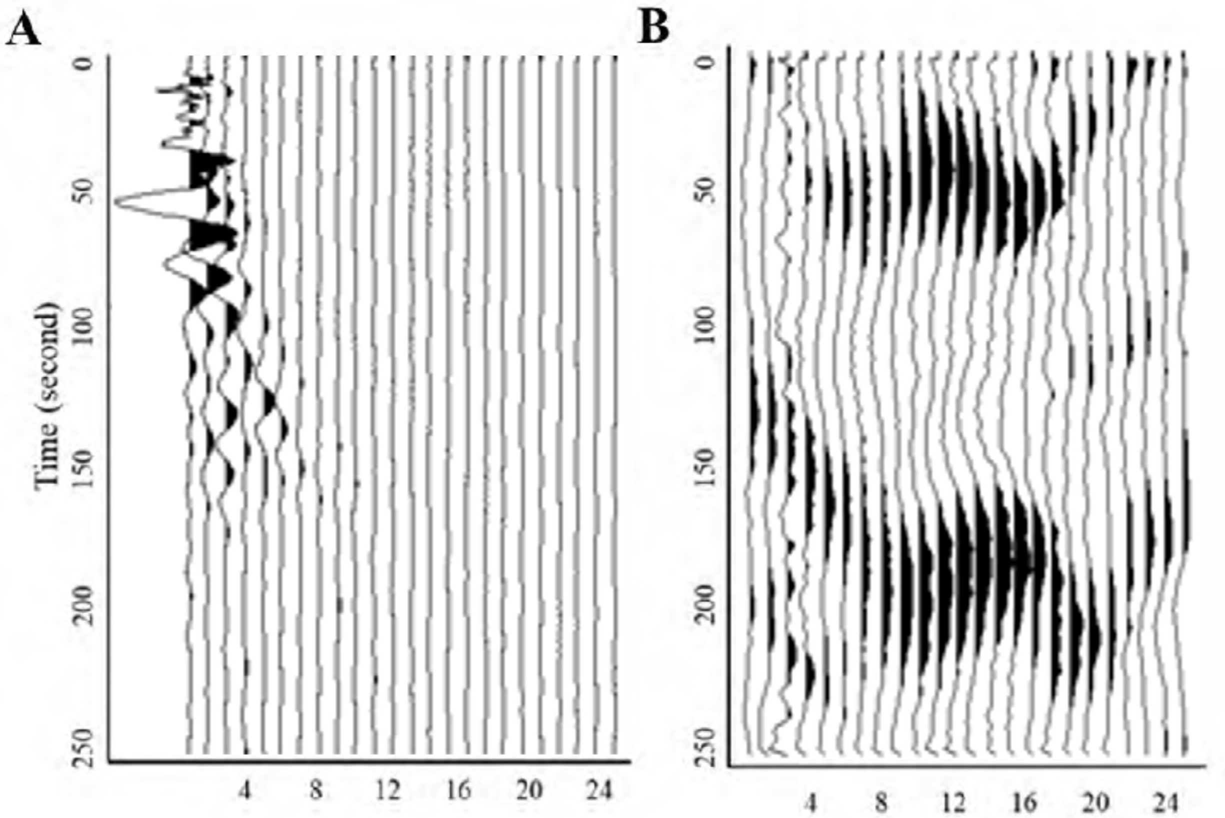

Figure 7. Raw seismic records for (A) the active multichannel analysis of surface wave (MASW) survey and (B) the passive MASW survey at Site 2

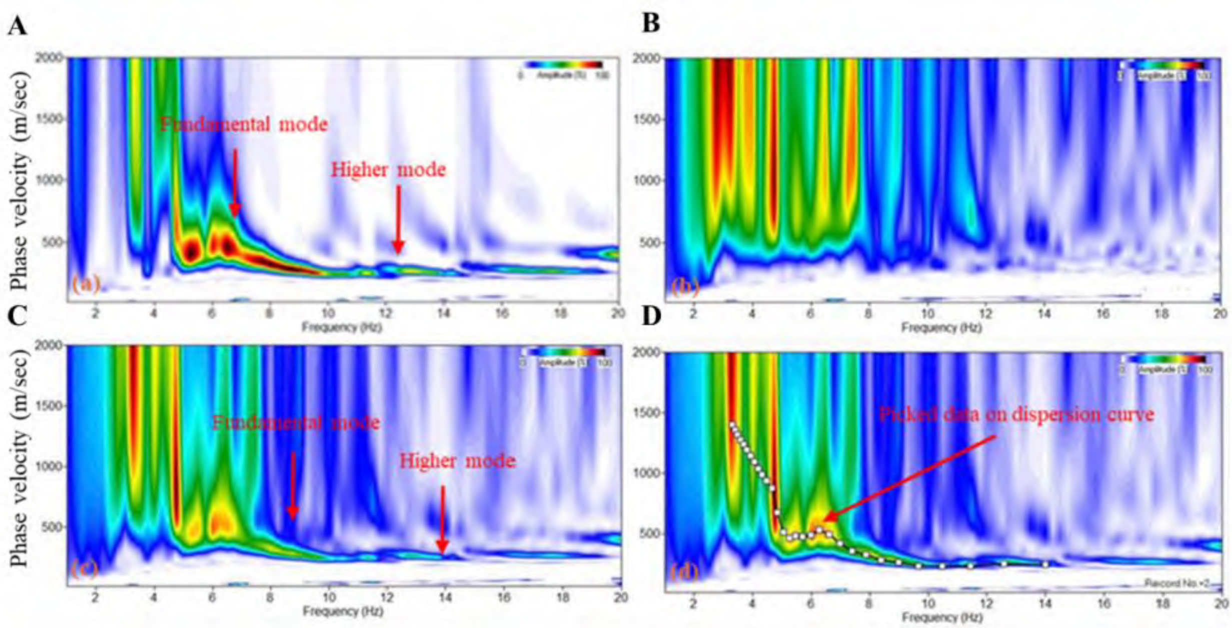

Figure 8. Dispersion images from Site 2. (A) Active multichannel analysis of surface wave data. (B) Passive extended spatial autocorrelation data. (C) The stacked combined data. (D) The picked fundamental mode used for inversion.

The calculated key geotechnical parameters are summarized in Table 2. The speeds of 517 m/s (Site 1) and 408 m/s (Site 2) categorize the area as National Earthquake Hazards Reduction Program (NEHRP) Site Class C ("very dense soil and soft rock"). The predominant ground period was relatively short (0.257 s to 0.322 s).

Subsequently, the dynamic shear modulus was mapped with depth (Figure 10), reflecting sharp lithological contrasts within the subsurface.

4. Discussion

4.1. Methodological efficacy and stratigraphic correlation

The successful generation of 1D profiles reaching 50 m depth validates our primary methodological hypothesis: integrating ESPAC passive data with active MASW

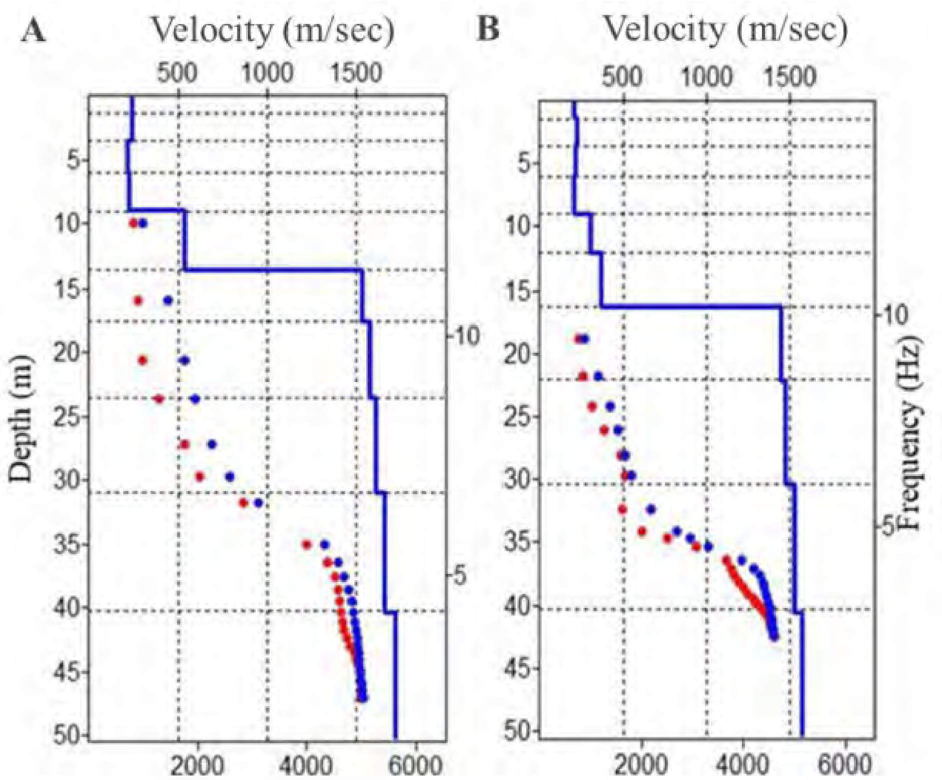

Figure 9. Obtained one-dimensional shear wave velocity structures with depth (blue lines), showing theoretical (blue dots) and measured (red dots) dispersion curves converging with an RMSE < 5% at (A) Site 1 and (B) Site 2

Table 2. Summary of calculated geotechnical parameters derived from the one-dimensional V_s profiles at Site 1 and Site 2

Survey site	Time-averaged shear wave velocity, V_{s30} (m/s)	Ground predominant period, T_s (s)	Maximum shear modulus, G_{max} (MPa)	NEHRP site classification	Estimated depth to bedrock (m)
Site 1	517	0.257	~7,400	Class C (very dense soil and soft rock)	10–15
Site 2	408	0.322	~6,620	Class C (very dense soil and soft rock)	10–15

Abbreviation: NEHRP: National Earthquake Hazards Reduction Program.

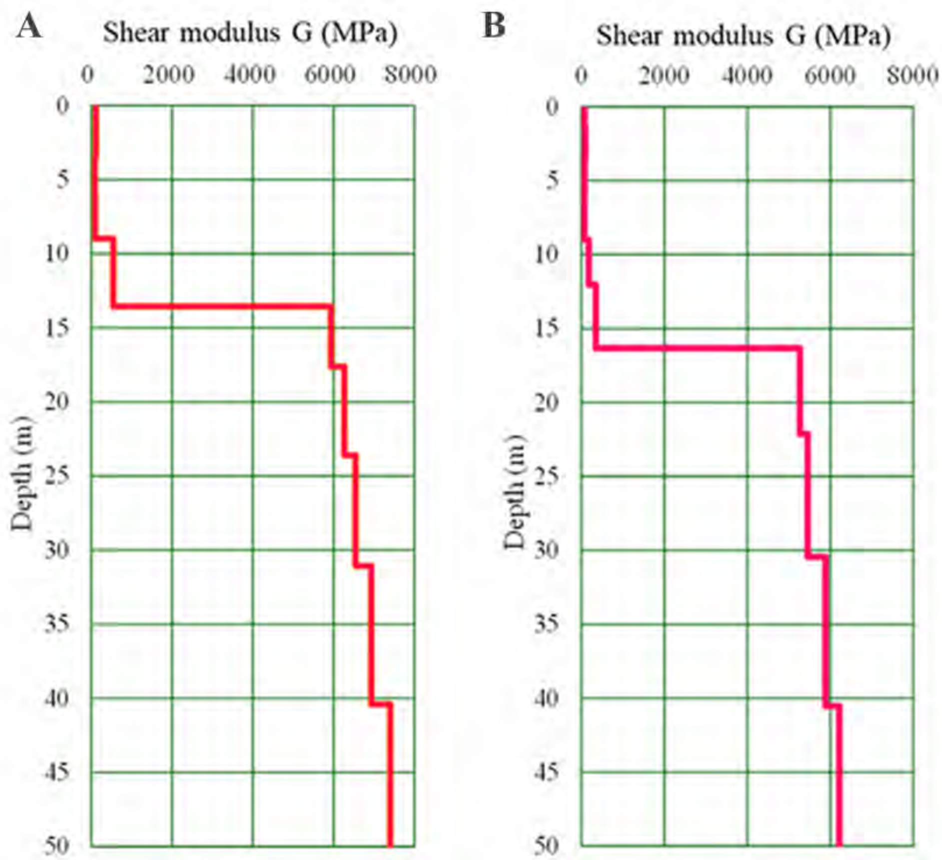

Figure 10. One-dimensional dynamic shear modulus profiles at (A) survey site 1 and (B) survey site 2, illustrating the sharp impedance contrasts

overcomes the physical limitations of standalone surveys in urban environments.[8,9] The issue of non-uniqueness in the inversion was effectively mitigated by anchoring the initial model with robust a priori borehole constraints.

The 1D and shear modulus profiles align perfectly with the reference borehole logs. We can divide the subsurface into three distinct geotechnical units:

- The overburden (0–10 m): Low velocities (m/s) and low shear moduli (MPa). This matches the semi-stiff clayey soils.
- The transition zone (10–15 m): A sharp velocity gradient where the velocity increases rapidly from 300 to 550 m/s. This represents the weathered interface.
- The bedrock (>15 m): Skyrockets to 1,400–1,700 m/s. This extreme stiffness signature is the definitive geophysical fingerprint of the fractured Bac Son limestone formation.

4.2. Contextual analysis of geohazard susceptibility

While the NEHRP Class C designation implies a generally stable macro-environment, relying solely on the designation masks a localized threat. The most vital finding of this study is the identification of the extreme impedance contrast occurring at approximately 15 m depth. The stratigraphic architecture—a 10 m layer of relatively soft clay atop a highly rigid, fractured limestone bedrock—is the classic prerequisite for karst subsidence.[31,32] The fractured limestone acts as an efficient subterranean aquifer. During extreme weather events, such as the heavy rainfall induced by Typhoon Yagi,[28] surface water rapidly infiltrates the clay layer. When this downward hydraulic gradient reaches the fractured bedrock interface, it triggers internal erosion or "piping" (Figure 11). The flowing groundwater washes fine clay particles into the limestone voids, creating subsurface cavities that may eventually breach the surface as sinkholes. While MASW primarily identifies subsurface stiffness contrasts rather than directly predicting failure, the sharp transition from low to extremely high delineates the exact zone of highest vulnerability. These findings strongly resonate with well-documented karst subsidence and landslide environments globally, including railway hazard cases and high-resolution karst mapping in China,[31-33] reinforcing the utility of combined MASW profiling as a

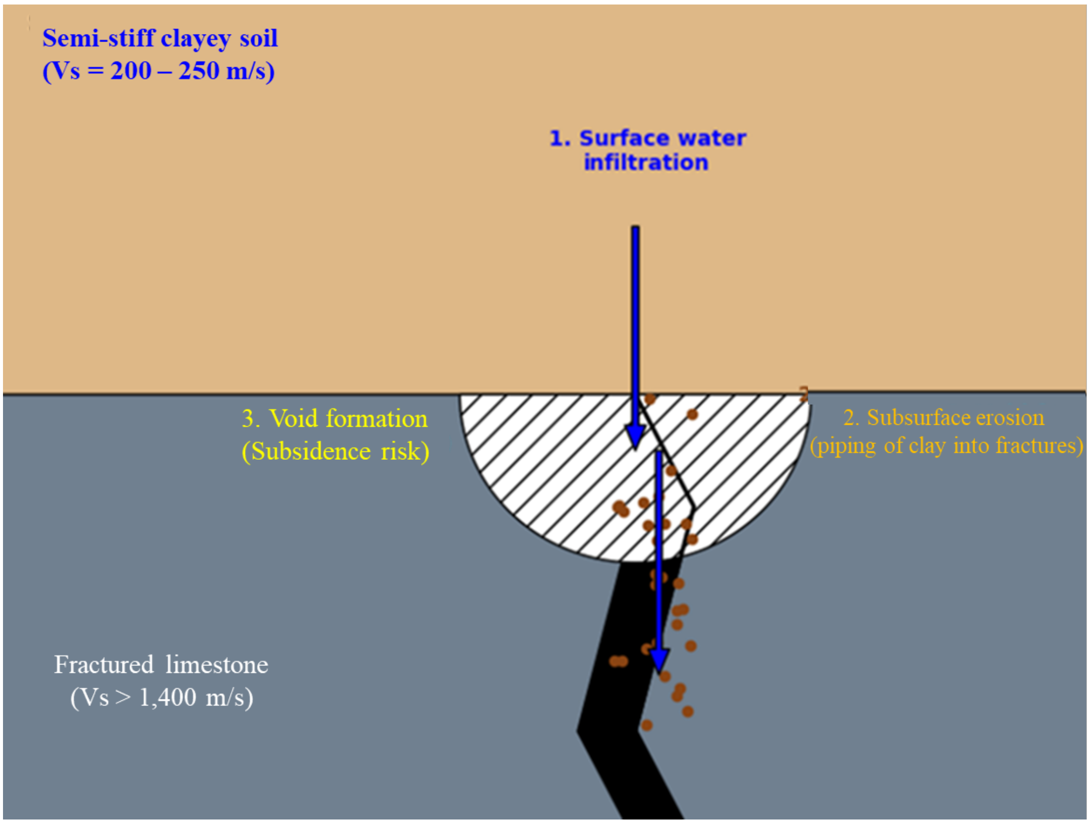

Figure 11. Conceptual model illustrating the mechanism of internal erosion (piping) at the sharp interface between the unconsolidated clay overburden and the fractured limestone bedrock
Abbreviation: Vs: Velocity.

reliable proxy for evaluating geohazard susceptibility.

5. Conclusion

This study establishes the combined active and passive (ESPAC) MASW as a highly effective, non-destructive diagnostic tool for deep subsurface characterization. By merging high-frequency hammer-impact data with low-frequency ambient noise using a fixed 69 m linear array, we successfully extracted broadband dispersion curves (2 Hz to 11 Hz) in Quang Hanh, Vietnam. This integrated approach enabled us to invert reliable 1D shear wave velocity profiles extending to 50 m in depth.

Our geophysical findings perfectly mirror the local geological reality. The true engineering value of this research lies in identifying the sharp, shallow impedance contrast between the clay overburden and the fractured bedrock (~15 m depth). This interface represents a critical zone of susceptibility to internal erosion (piping) and localized slope instability. We recommend that future infrastructure projects in this transitional karst terrain utilize these profiles as a crucial baseline, prioritizing deep piling anchored securely into the limestone layer to mitigate severe subsidence risks.

Acknowledgments

The authors would like to thank the Department of Seismology, Institute of Earth Sciences, Viet Nam Academy of Science and Technology, Ha Noi City, Vietnam, for their technical support during the MASW data acquisition.

Funding

This research is funded by Vietnam National University Ho Chi Minh City (VNU-HCM) under a project (grant number CB2025-18-11) within the framework of the Program titled "Strengthening the capacity for education and basic scientific research integrated with strategic technologies at VNU-HCM, aiming to achieve advanced standards comparable to regional and global levels during the 2025–2030 period, with a vision toward 2045."

Conflict of interest

The authors declare that they have no known competing financial interests or personal relationships that could have appeared to influence the work reported in this paper.

Author contributions

Conceptualization: Nguyen N. K. Ngan, Nguyen V. Thuan
Formal analysis: Nguyen T. Hai, Nguyen V. Thuan
Investigation: Nguyen T. Hai
Methodology: Nguyen T. Hai, Nguyen V. Thuan
Writing–original draft: Nguyen N. K. Ngan, Nguyen V. Thuan
Writing–review & editing: Nguyen N. K. Ngan, Nguyen V. Thuan

Availability of data

The raw data supporting the findings of this study are available from the corresponding author upon reasonable request.

References

1. Park CB, Miller RD, Xia J. Multichannel analysis of surface waves. *Geophysics*. 1999;64(3):800-808.

   doi: 10.1190/1.1444590

2. Taipodia J, Dey A. A review of active and passive MASW techniques. In: *Proceedings of the National Workshop on Engineering Geophysics for Civil Engineering and Geo-Hazards (EGCEG 2012)*; 2012; Roorkee, India. Accessed May 19, 2026. https://www.researchgate.net/publication/280977953_A_Review_of_Active_and_Passive_MASW_Techniques

3. Park CB, Miller RD, Xia J, Ivanov J. Multichannel analysis of surface waves (MASW)-active and passive methods. *Leading Edge*. 2007;26(1):60-64.

   doi: 10.1190/1.2431832

4. Okada H, Suto K. *The Microtremor Survey Method*. Tulsa, OK: Society of Exploration Geophysicists; 2003.

   doi: 10.1190/1.9781560801740

5. Asten MW. On bias and noise in passive seismic data from finite circular array data processed using SPAC methods. *Geophysics*. 2006;71(6):V153-V162.

   doi: 10.1190/1.2345054

6. Morton SL, Ivanov J, Peterie SL, Miller RD, Livers-Douglas AJ. Passive multichannel analysis of surface waves using 1D and 2D receiver arrays. *Geophysics*. 2021;86(6):EN63-EN75.

   doi: 10.1190/geo2020-0104.1

7. Eikmeier CN, Prado RL, Taioli F. Combined use of active and passive surface waves for shallow subsurface investigation in noisy urban area of Sao Paulo City, Brazil. *Rev Bras Geofís*. 2016;34(1):13-24.

   doi: 10.22564/rbgf.v34i1.779

8. Park CB, Miller RD, Ryden N, Xia J, Ivanov J. Combined use of active and passive surface waves. *J Environ Eng Geophys*. 2005;10(3):323-334.

   doi: 10.2113/jeeg10.3.323

9. Lontsi AM, Ohrnberger M, Kruger F. Shear wave velocity profile estimation by integrated analysis of active and passive seismic data from small aperture arrays. *J Appl Geophys*. 2016;130:37-52.

   doi: 10.1016/j.jappgeo.2016.03.034

10. Cheng F, Xia J, Luo Y, *et al*. Multichannel analysis of passive surface waves based on crosscorrelations. *Geophysics*. 2016;81(5):EN57-EN66.

    doi: 10.1190/geo2015-0505.1

11. Mahajan AK, Galiana-Merino JJ, Lindholm C, *et al*. Characterization of the sedimentary cover at the Himalayan foothills using active and passive seismic techniques. *J Appl Geophys*. 2011;73(3):196-206.

    doi: 10.1016/j.jappgeo.2011.01.002

12. Malovichko AA, Anderson NL, Malovichko DA, Shylakov DY, Butirin PG. Active-passive array surface wave inversion and comparison to borehole logs in southeast Missouri. *J Environ Eng Geophys*. 2005;10(3):243-250.

    doi: 10.2113/jeeg10.3.243

13. Ariffin J, Ismail MAM, Tan CG, Murtadza NM. Site characterization of marine clay deposits in South Seberang Prai, Penang using combined active and passive multichannel analysis of surface wave (MASW). *IOP Conf Ser Mater Sci Eng*. 2016;136:012032.

    doi: 10.1088/1757-899X/136/1/012032

14. Ning L, Dai T, Liu Y, Xi C, Zhang H, Zhou C. Application of multichannel analysis of passive surface waves method for fault investigation. *J Appl Geophys*. 2021;192:104382.

    doi: 10.1016/j.jappgeo.2021.104382

15. Hu S, Zhao Y, Ma Z, *et al*. Combined analysis of active and passive surface waves for 2D characterization of a landfill. *J Appl Geophys*. 2022;206:104832.

    doi: 10.1016/j.jappgeo.2022.104832

16. Widyaningrum Y, Sungkono S, Husein A, Santosa BJ, Bahri AS. Combination of active and passive seismic analyses for embankment characterization. *Appl Mech Mater*. 2015;771:179-182.

    doi: 10.4028/www.scientific.net/AMM.771.179

17. Karsli H, Babacan AE, Akin O. Subsurface characterization by active and passive source geophysical methods after the 06 February 2023 earthquakes in Turkey. *Nat Hazards*. 2024;120(6):5257-5286.

    doi: 10.1007/s11069-024-06422-6

18. Adly A, Poggi V, Fah D, Hassoup A, Omran A. Combining

active and passive seismic methods for the characterization of urban sites in Cairo, Egypt. *Geophys J Int*. 2017;210(1):428-442.

doi: 10.1093/gji/ggx176

19. Budi AP, Ginting RA, Sunardi B, Sukanta IN. Combination of passive seismic (HVSR) and active seismic (MASW) methods to obtain shear wave velocity model of subsurface in Majalengka. *J Phys Conf Ser*. 2021;1805(1):012002.

    doi: 10.1088/1742-6596/1805/1/012002

20. Eker AM, Akgun H, Kockar MK. A comparison of local site conditions with passive and active surface wave methods. In: *Proceedings of the Fifth International Conference on Recent Advances in Geotechnical Earthquake Engineering and Soil Dynamics*; May 24-29, 2010; San Diego, CA. Accessed May 19, 2026. https://scholarsmine.mst.edu/icrageesd/05icrageesd/session06b/1/

21. Eker AM, Akgun H, Kockar MK. Local site characterization and seismic zonation study by utilizing active and passive surface wave methods: a case study for the northern side of Ankara, Turkey. *Eng Geol*. 2012;151:64-81.

    doi: 10.1016/j.enggeo.2012.09.002

22. Ladak S, Molnar S, Palmer S, Atkinson GM. Application of active and passive seismic methods for determining the shear wave velocity profile at hard rock sites in Eastern Canada. In: *Proceedings of the 12th Canadian Conference on Earthquake Engineering*; 2019; Quebec City, QC, Canada. Accessed May 19, 2026. https://www.caee.ca/12CCEEpdf/192-bN89-149.pdf

23. Philley PD, Taipodia J, Pana T. Subsurface investigation analysis using combined MASW survey. In: *Proceedings of the Indian Geotechnical Conference 2022*. Lecture Notes in Civil Engineering. Singapore: Springer Nature; 2024:313-324.

    doi: 10.1007/978-981-97-1737-8_27

24. Zaki MFM, Ghazaly ZM, Bawadi NF, Ahmad MM, Nujid MM. Indicative microzonation map of the contact zone between the Kenny Hill and limestone formation using active, passive and hybrid MASW methods. *IOP Conf Ser Earth Environ Sci*. 2024;1369(1):012023.

    doi: 10.1088/1755-1315/1369/1/012023

25. Abdelbaset M, Mohamed A, Sawires R, Omran AAA, Thabet M. Passive and active seismics to identify geotechnical site characterization at industrial zone, Aswan, Egypt. *J Appl Geophys*. 2025;243:105948.

    doi: 10.1016/j.jappgeo.2025.105948

26. Nguyen NKN. Deriving geotechnical parameters for foundation design in Ea Trang, Vietnam, through combined seismic methods. *Econ Environ Geol*. 2025;58(4):351-359.

    doi: 10.9719/eeg.2025.58.4.351

27. Nguyen NNK, Le CVA, Vu TM, *et al*. Determination of shear wave velocity using multichannel analysis of surface wave in M'Drak District, Dak Lak Province, Vietnam. *IEEJ Trans Electr Electron Eng*. 2025;20(11):1896-1900.

    doi: 10.1002/tee.70089

28. Nguyen TH. Consulting, survey and overall assessment of areas at risk of subsidence, sliding, and landslide after Typhoon Yagi in Quang Hanh Ward, Cam Pha City, Quang Ninh Province. Technical report. Department of Seismology, Institute of Earth Sciences, Viet Nam Academy of Science and Technology; 2024.

29. Akin O, Sayil N. Soil characterization in landslide-prone areas using ground shear strain based on active and passive source surface wave methods. *Pure Appl Geophys*. 2025;182(4):1579-1600.

    doi: 10.1007/s00024-025-03696-0

30. Hayashi K, Suzuki H. CMP cross-correlation analysis of multi-channel surface-wave data. *Explor Geophys*. 2004;35(1):7-13.

    doi: 10.1071/EG04007

31. Wang Z, Juhlin C, Lu Q, *et al*. High-resolution seismic reflection surveying to delineate shallow subsurface geological structures in the karst area of Shenzhen, China. *Solid Earth*. 2025;16(8):761-773.

    doi: 10.5194/se-16-761-2025

32. Wang Z, Zhu T. Characterizing fractured zones in urban karst geology using leaky surface waves from distributed acoustic sensing. *J Geophys Res Solid Earth*. 2025;130(7):e2025JB031477.

    doi: 10.1029/2025JB031477

33. Islam N, Xu L, Usman AB, Raza B, Li Y, Li S. Study on field and numerical analysis of karst collapse as railway hazard. *Proc Inst Civ Eng Geotech Eng*. 2025;178(3):324-338.

    doi: 10.1680/jgeen.24.00242